Journal of ELECTRONIC MATERIALS, Vol. 47, No. 10, 2018
https://doi.org/10.1007/s11664-018-6172-2
© 2018 The Minerals, Metals & Materials Society

U.S. WORKSHOP ON PHYSICS AND CHEMISTRY OF II-VI MATERIALS 2017

Inductively Coupled Plasma-Induced Electrical Damage on HgCdTe Etched Surface at Cryogenic Temperatures

L.F. LIU,[1,2] Y.Y. CHEN,[1,2] Z.H. YE,[1,3] X.N. HU,[1] R.J. DING,[1] and L. HE[1]

1.—Key Laboratory of Infrared Imaging Materials and Detectors, Shanghai Institute of Technical Physics, Chinese Academy of Sciences, Shanghai 200083, China. 2.—University of Chinese Academy of Sciences, Beijing 100039, China. 3.—e-mail: zhye@mail.sitp.ac.cn

Plasma etching is a powerful technique for transferring high-resolution lithographic patterns into HgCdTe material with low etch-induced damage, and it is important for fabricating small-pixel-size HgCdTe infrared focal plane array (IRFPA) detectors. *P*- to *n*-type conversion is known to occur during plasma etching of vacancy-doped HgCdTe; however, it is usually unwanted and its removal requires extra steps. Etching at cryogenic temperatures can reduce the etch-induced type conversion depth in HgCdTe via the electrical damage mechanism. Laser beam-induced current (LBIC) is a nondestructive photoelectric characterization technique which can provide information regarding the vertical and lateral electrical field distribution, such as defects and *p*–*n* junctions. In this work, inductively coupled plasma (ICP) etching of HgCdTe was implemented at cryogenic temperatures. For an Ar/CH_4 (30:1 in SCCM) plasma with ICP input power of 1000 W and RF-coupled DC bias of $\sim$ 25 V, a HgCdTe sample was dry-etched at 123 K for 5 min using ICP. The sample was then processed to remove a thin layer of the plasma-etched region while maintaining a ladder-like damaged layer by continuously controlling the wet chemical etching time. Combining the ladder etching method and LBIC measurement, the ICP etching-induced electrical damage depth was measured and estimated to be about 20 nm. The results indicate that ICP etching at cryogenic temperatures can significantly suppress plasma etching-induced electrical damage, which is beneficial for defining HgCdTe mesa arrays.

Key words: HgCdTe, MCT, inductively coupled plasma (ICP) etching, cryogenic etching, cryoetching, etch-induced electrical damage, laser beam-induced current (LBIC)

INTRODUCTION

HgCdTe is one of the most important infrared materials, and has been commonly used for a wide range of infrared detection applications since it was first synthesized in the early 1960s. Third-generation HgCdTe-based infrared focal plane array (IRFPA) detectors of increasing device complexity, including megapixel format arrays, small pixel sizes, and dual-band or even multispectral capabilities, have given rise to tremendous chip processing challenges during device fabrication.[1] For instance, to accurately transfer high-resolution lithographic patterns into HgCdTe, a highly anisotropic etching process with low damage for high-aspect-ratio trench fabrication would be indispensable. To realize these novel structures, dry processes such as ion beam etching (IBE)[2,3] and plasma etching began to replace wet chemical processes, which were normally isotropic and not environmentally friendly.[4] High-density plasma processes such as electron cyclotron resonance (ECR) and inductively coupled plasma (ICP)-enhanced reactive ion

(Received November 10, 2017; accepted February 22, 2018; published online March 12, 2018)

etching have been intensively studied. ICP has now become the main tool for processing of HgCdTe.[5–9] However, plasma processes often lead to HgCdTe surface lattice damage and deterioration of electrical properties due to the material's low damage threshold.

P- to *n*-type conversion on the etched surface of vacancy-doped HgCdTe is known to occur during the dry etching process, and this is typically undesired.[2,10] Wet etching and annealing processes have been widely used to remove the thin conversion surface layer after the dry etch process.[11,12] It was also reported that cooling of the substrate to temperatures around 100 K during the etching process can suppress the Hg interstitial diffusion process responsible for the *p*-to-*n* conversion.[10,13] The results showed that lowering the temperature of the sample during the plasma process can suppress the *p*-to-*n* conversion.

In this paper, a HgCdTe sample with four columns of array patterns was etched at 123 K using ICP, after which the sample underwent wet processing to remove a ladder-like layer of HgCdTe as described in the next section. Combining the wet process and laser beam-induced current (LBIC) measurement, the *p*-to-*n* conversion depth was determined quantitatively.

EXPERIMENT DETAILS

The experimental studies in this paper were performed on liquid-phase epitaxy (LPE)-grown $x = 0.22$ vacancy-doped *p*-type HgCdTe. An approximately $1 \times 1\ \text{cm}^2$ sample was patterned with 4 rows × 5 columns of square arrays (10 × 10 50 μm × 50 μm squares array), as shown in Fig. 1. A Plasmalab System 100 system (Oxford Instruments, Abingdon, UK) with a liquid nitrogen cooling set was used for HgCdTe etching. This system has one RF-coupled DC biasing source, with input power ranging from 0 W to 300 W, and one plasma generator with power ranging from 0 W to 2000 W. The substrate temperature can be cooled to 123 K. A CH_4/Ar = 1/30 (total in SCCM) gas mixture, ICP power of 1000 W, RF power of 10 W, and a total chamber pressure of 6.65×10^{-1} Pa were employed for etching of HgCdTe. The sample was glued on a 3-inch Si wafer and etched for 5 min with an etching depth of about 1.1 μm at 123 K. The mask was then removed, and the etched region was processed to remove a ladder-like part using 0.5% bromine/hydrobromic acid with a maximal depth of 500 nm, as illustrated in Fig. 2. The sample was subsequently covered with 73 nm ZnS, electrical contacts were made on both sides of the sample, and LBIC was employed to evaluate the *p*-to-*n* conversion region in the HgCdTe epilayer. LBIC is a nondestructive optical characterization technique which can be used to investigate electrically active regions and has been used previously in HgCdTe characterization.[14,15]

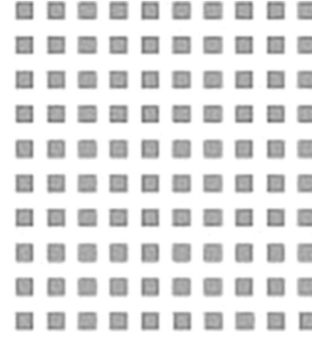

Fig. 1. Illustration of the 10 × 10 50 μm × 50 μm square array.

RESULTS AND DISCUSSION

A typical LBIC signal profile of a *p*–*n* junction is shown in Fig. 3. When a focused laser beam scans a *p*–*n* junction, photo-generated electron–hole pairs are separated by the built-in electric field, which results in an induced photocurrent as a function of incident laser beam position. The magnitude and direction of the current depends on the position of the laser beam relative to the local field configuration.[15] The inflection point in the LBIC signal profile locates the junction position. The width of the *n* region is defined by the mask pattern, which is 50 μm × 50 μm square in our case. If the LBIC signal showed no inflection point with the period of the pattern, it would suggest that the *n* region has been completely removed. As shown in Fig. 4, the LBIC signal disappears at the first 50 μm × 50 μm square, which means the *n* region has been completely removed at the second square and partially removed at the first square. The depth of the first square was then measured using a Dektak 150 profilometer (Veeco Instruments Inc., Plainview, NY, USA), and the *p*-to-*n* conversion depth was estimated to be about 20 nm.

During the ICP etching process, accelerated plasma ions sputter the vacancy-doped *p*-type HgCdTe surface, liberating Hg interstitials under the etched surface. The rapid diffusion of Hg interstitials into the material decreases the concentration of acceptors by interaction with point defects, mainly Hg vacancies. As a result, an *n*-type region with dominating residual uncompensated donors is created.[10]

Considering that the Hg diffusion process is the main reason for *p*- to *n*-type conversion during ICP etching, the speed at which Hg interstitials diffuse determines the final depth of the etch-induced *n* region. The *n* conversion depth d, and the Hg interstitial diffusion coefficient D_I can be expressed as follows[13]:

$$d = \alpha\sqrt{D_I t}, \tag{1}$$

$$D_I = D_0 \exp\left(-\frac{E_M}{k_B T}\right), \tag{2}$$

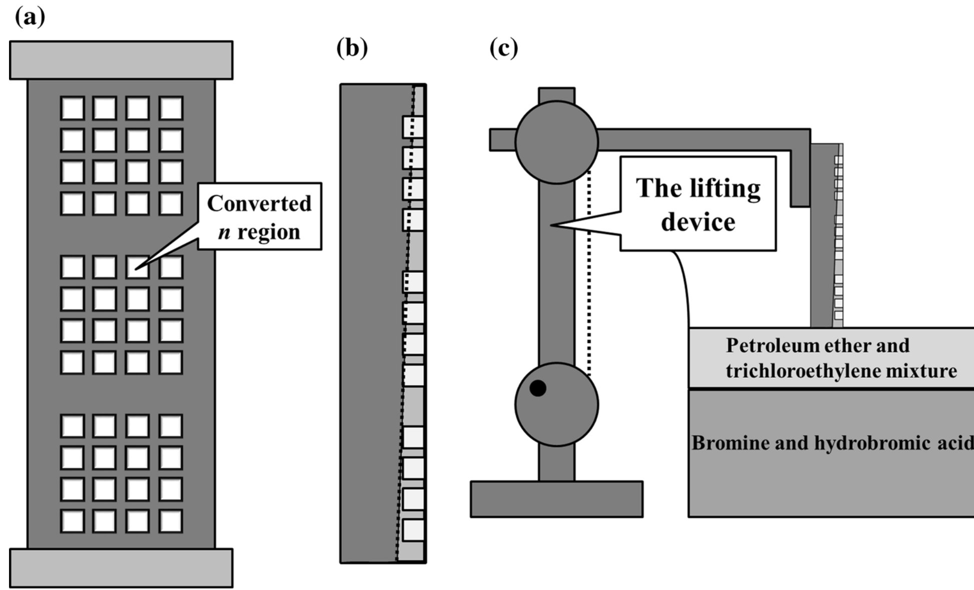

Fig. 2. (a) A front-view illustration of the etched sample, where the white area represents the converted *n* region, and (b) a side view illustration of the etched sample. The region to the right of the dotted line is removed by wet processing. (c) An illustration of the wet processing device. (For simplicity, the patterns shown are not the actual patterns on the sample).

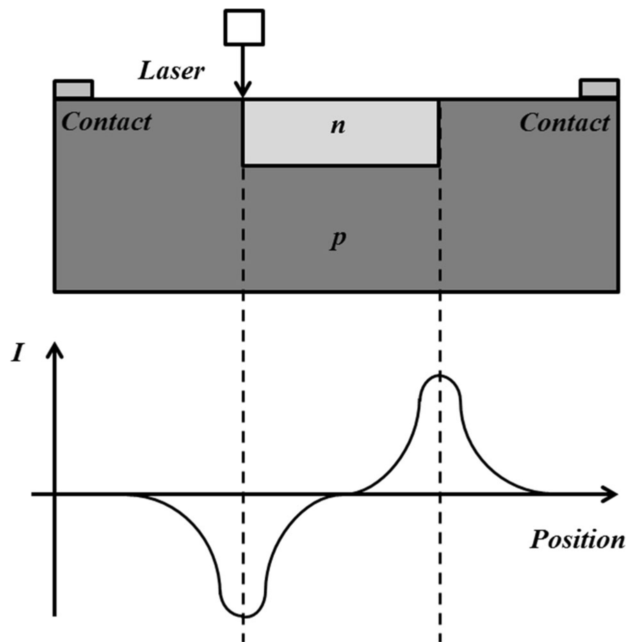

Fig. 3. The principle of planar *n*-on-*p* junction LBIC testing.

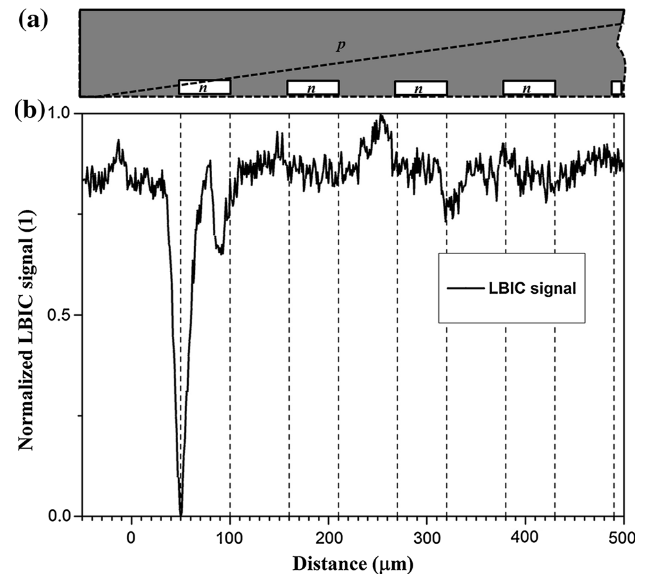

Fig. 4. (a) An illustration of the converted *n* region of the ICP etched sample. The area surrounded by dashed lines represents the region being removed by the wet process. (b) LBIC signal of the ICP etched sample after the wet process. Dashed lines serve as guidelines for the ICP etched area, i.e. the *p*–*n* junction position.

where α and D_0 are constants. T, t, E_{M} and k_{B} are the sample temperature, the etch time, the migration energy of Hg interstitials and the Boltzmann constant, respectively.

It has been reported that the value of $E_{\mathrm{M}} = 120 \pm 30$ meV.[13] For $E_{\mathrm{M}} = 90$ meV, the ratio of d at 300 K to d at 123 K is $\frac{d|_{300\,\mathrm{K}}}{d|_{123\,\mathrm{K}}} = \sqrt{\frac{D_I|_{300\,\mathrm{K}}}{D_I|_{123\,\mathrm{K}}}}$ $= \sqrt{\exp\left[\frac{9\times10^{-2}\,\mathrm{eV}}{8.617} \times 10^{-5}\,\mathrm{eV\,K^{-1}}\right] \left(\frac{1}{123\,\mathrm{K}} - \frac{1}{300\,\mathrm{K}}\right)} \approx 10.$

For $d|_{123\,\mathrm{K}} = 20$ nm, as we measured, $d|_{300\,\mathrm{K}}$ would be about 200 nm; for $E_M = 150$ meV, $\frac{d|_{300\,\mathrm{K}}}{d|_{123\,\mathrm{K}}} = \sqrt{\frac{D_I|_{300\,\mathrm{K}}}{D_I|_{123\,\mathrm{K}}}} = \sqrt{\exp\left[\frac{1.5\times10^{-1}\,\mathrm{eV}}{8.617\times10^{-5}\,\mathrm{eV\,K^{-1}}}\right] \left(\frac{1}{123\,\mathrm{K}} - \frac{1}{300\,\mathrm{K}}\right)} \approx$ 65, $d|_{300\,\mathrm{K}}$ would be about 1300 nm. Thus temperature has a significant influence on the conversion depth, especially for cases with higher E_{M}, and the speed of the conversion process can be reduced with a smaller D_I at lower temperatures. Hence, ICP

etching at cryogenic temperatures helps to reduce the damage to the surface of an HgCdTe film.

CONCLUSION

The influence of temperature on the etch-induced *p*- to *n*-type conversion depths of HgCdTe at 123 K was investigated using ICP. Combining the wet process and LBIC technique, the conversion depth at 123 K was estimated to be about 20 nm. The *p*-to-*n* conversion process during ICP etching can be suppressed at cryogenic temperatures, which is beneficial for the process of IRFPA device fabrication.

CONFLICT OF INTEREST

The authors declare that they have no conflict of interest.

REFERENCES

1. A. Rogalski, J. Antoszewski, and L. Faraone, *J. Appl. Phys.* 105, 4 (2009).
2. JTM Wotherspoon, U.K. Patent No. GB2095898 (1981).
3. M.V. Blackman, D.E. Charlton, M.D. Jenner, D.R. Purdy, J.T.M. Wotherspoon, C.T. Elliott, and A.M. White, *Electron. Lett.* 23, 978 (1987).
4. V. Srivastav, R. Pal, and H.P. Vyas, *Opto-Electron. Rev.* 13, 197 (2005).
5. C.R. Eddy, E.A. Dobisz, J.R. Meyer, and C.A. Hoffman, *J. Vac. Sci. Technol. A* 11, 1763 (1993).
6. A.J. Stoltz, J.D. Benson, P.R. Boyd, M. Martinka, J.B. Varesi, A.W. Kaleczyc, E.P.G. Smith, S.M. Johnson, W.A. Radford, and J.H. Dinan, *J. Electron. Mater.* 32, 692 (2003).
7. E. Laffosse, J. Baylet, J.P. Chamonal, G. Destefanis, G. Cartry, and C. Cardinaud, *J. Electron. Mater.* 34, 740 (2005).
8. E.P.G. Smith, J.K. Gleason, L.T. Pham, E.A. Patten, and M.S. Welkowsky, *J. Electron. Mater.* 32, 816 (2003).
9. A.J. Stoltz, J.D. Benson, and P.J. Smith, *J. Electron. Mater.* 37, 1225 (2008).
10. E. Belas, J. Franc, A. Toth, P. Moravec, R. Grill, H. Sitter, and P. Höschl, *Semicond. Sci. Technol.* 11, 1116 (1996).
11. E.P.G. Smith, J.F. Siliquini, C.A. Musca, J. Antoszewski, J.M. Dell, L. Faraone, and J. Piotrowski, *J. Appl. Phys.* 83, 5555 (1998).
12. A. Gaucher, J. Baylet, J. Rothman, E. Martinez, and C. Cardinaud, *J. Electron. Mater.* 42, 3006 (2013).
13. E. Belas, R. Grill, J. Franc, A. Toth, P. Hoschl, H. Sitter, and P. Moravec, *J. Cryst. Growth* 159, 1117 (1996).
14. J. Bajaj, L.O. Bubulac, P.R. Newman, W.E. Tennant, and P.M. Raccah, *J. Vac. Sci. Technol. A* 5, 3186 (1987).
15. W.C. Qiu, X.A. Cheng, R. Wang, Z.J. Xu, and T. Jiang, *J. Appl. Phys.* 115, 204506 (2014).